Performance Analysis of a Doubly Excited Brushless Machine for Variable Speed Application

Huijuan Liu[1], Longya Xu[2]
[1] School of Electrical Engineering, Beijing Jiaotong University, Beijing, 100044, China
[2] Department of Electrical & Computer Engineering, The Ohio State University, Columbus, Ohio 43210, USA
E-mail: hiliu@bitu.edu.cn

Abstract — A novel doubly excited brushless machine (DEBM) with the radially laminated magnetic barrier rotor (RLMB-rotor) for variable speed system is built, and the prototype machine of 250kW/1200rpm has 10 rotor pole numbers. The performance studies of the sample machine are presented by using the 2D transient finite element analysis model and the experimental method. The magnetic fields, the electromagnetic torque characteristics of the prototype machine are investigated. The experiment results validate the theoretical analysis results and all studies show that the prototype RLMB-rotor DEBM is potential to apply in variable speed system.

I. INTRODUCTION

With the development of the power electronics converter in recent years, doubly excited brushless machines (DEBMs) have gained deserved attention in the applications of variable-speed constant-frequency generating and adjustable speed drive systems [1-7]. A DEBM appears very attractive for its rugged structure (complete absence of slip rings and brushes), good compatibility with power converter, and flexible operational modes for various application needs. In particular, DEBMs resemble the terminal characteristics of a wound rotor doubly excited induction machine. This has made DEBM a very competitive candidate in applications where doubly fed operational modes are deemed appropriate but slip rings and brushes not allowed [8-12].

The DEBM has two sets of separate windings with different pole numbers located on the stator, and the rotor is structured with several reluctance segments (or nested shorted-circuits) with pole number different from either of the stator windings. Previous investigations on rotor styles indicated that the rotor style has strong effects on the rotor modulation capabilities. In past research activities, [1-9] conducted detailed investigation and presented throughout analysis on the magnetic coupling between the two stator windings with different rotor structures. The research work shows that a DEBM with radial laminations and axial flux barriers rotor has much better magnetic coupling and torque performance than those with other rotor types [4, 5, 6]. In addition to the rotor style and laminations design, we also found that the combinations of the DEBM pole number are of great influence to the rotor modulation and, thus, to the mutual coupling of the two stator windings.

The paper starts with a brief review of main configuration and basic principles of DEBM and system. Then, using finite element analysis, the magnetic fields distribution, the torque and the terminal characteristics of the prototype DEBM of 250kW/1200rpm are presented. The designed machine is built and tested in laboratory, and the experimental results are presented. Fig.1 shows the cross section of the prototype DEBM.

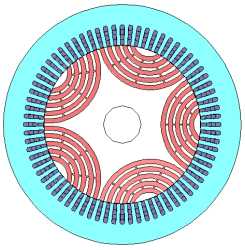

Fig. 1 Cross section of the DEBM

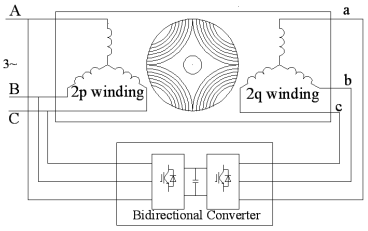

Fig. 2 Schematic diagram of a DEBM system

II. PERFORMANCE ANALYSIS BY FEM

A. The prototype Machine of DEBM with RLMB-rotor

As shown in Fig. 2, the DEBM system consists of three main components, a DEBM, a back-to-back inverter and an associated controller. DEBM is a controlled electric machine, meaning that for its practical applications, it is necessary to mate DEBM with a bidirectional power flow converter.

In the system, the stator of a DEBM has two sets of three-phase sinusoidal distributed windings. One set of windings, the primary, is connected directly to the power grid. The other set of windings, the secondary, is fed with variable voltages at variable frequencies from a converter that also is connected to the power grid. The two sets of windings differ in pole numbers, one of $2p$ and another $2q$. The rotor of the DEBM is a special design, with a group of magnetically isolated segments of number p_r where

$$p_r = p+q \qquad (1)$$

Eq. (1) indicates that the rotor segment number is constrained by the pole numbers of the two stator windings but among the three numbers we do have a degree of freedom of two. The operation of the DEBM relies on the interaction of the two stator windings through the intermediate action of the rotor. When one set of symmetrical sine-wave currents of frequency ω_1 are flowing in the primary windings, a set of three-phase back EMFs will be induced with a frequency of ω_2 in the secondary windings. The two electrical frequencies ω_1 and ω_2 are related to the rotor mechanical speed ω_{rm} by the following equation

$$\omega_{rm}=(\omega_1\pm\omega_2)/p_r \qquad (2)$$

Electromechanical energy conversion will take place in DEBMs if Eq. (2) is satisfied. Depending on the sequence and value of the controlled frequency ω_2, a DEBM can operate in different modes. In particular, in the doubly-excited mode with $\omega_2=0$, the DEBM is operated as a synchronous machine at natural synchronous speed. On the other hand, with $\omega_2>0$ or

ω_2<0 (negative sequence), a DEBM can operate as an induction machine below or above natural synchronous speed. In terms of power flow, regardless at the sub-, super-, or synchronous rotor speed, DEBM always can be operated as a motor or generator.

The sizing of the 250kw/1200rpm DEBM starts with a comparable and conventional doubly fed wound rotor induction machine. By try-and-error, the RLMB-rotor DEBM main dimensions are determined with the design specifications listed in Table 1. As summarized in Table I, the prototype DEBM is designed with two sets of stator windings, one for 6-pole and another 4-pole. The synchronous speed of the designed DEBM is 600 rpm and in order to deliver the rated power of 250kW, the DEBM is at the super synchronous speed of 1,200rpm. In operation, the primary winding of 6-pole will be connected to the power grid of 50Hz while the secondary winding of 4-pole will be controlled by a bi-directional converter, consisting of two inverters in back to back connection.

TABLE I MAIN DIMENSIONS

Rated Power (kW)	250	Rated Speed (rpm)	1200
Rated V_{line} (V)	690	Rated Freq. (Hz)	50
Rated I_P (A)	246	Primary winding	6-pole
Rated I_S (A)	246	Secondary winding	4-pole
Power Factor	controllable	Rotor Segments	5, 10-pole
Stator OD (mm)	740	Stator Slots	72
Stator ID (mm)	501	Stack Length (mm)	600
Rotor OD (mm)	499.4	Rotor ID (mm)	200

B. *Magnetic field distribution*

The mesh division of the sample RLMB-rotor DEBM is shown in Fig. 3. When two sets of stator winding is excited with a three-phase current at a frequency of interests, the sample machine will operate in load operation. The flux distribution over the cross-section of the sample RLMB-rotor DEBM in load operation is shown in Fig. 4. The magnetic field of the RLMB-rotor DEBM is not symmetric and calculation of the entire magnetic field for the DEBM is needed. The air-gap field distribution of the sample RLMB-rotor DEBM in load operation is shown in Fig. 5.

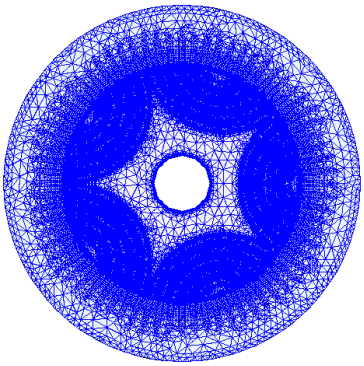

Fig. 3 Mesh division of the prototype DEBM

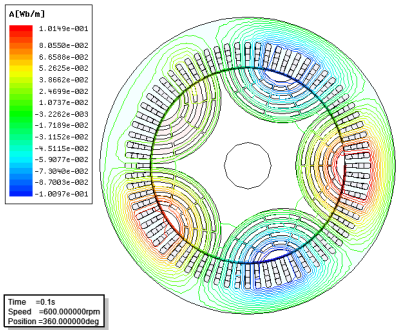

Fig. 4 Flux distribution

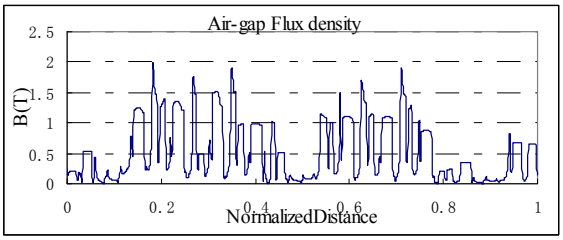

Fig. 5 Air-gap flux density distribution

C. *Winding flux linkages*

In the finite element analysis, we have directly calculated two types of flux linkages of the RLMB-rotor DEBM, i.e. the self- and the mutual-flux linkages. The advantages of direct computing flux linkage over computing inductance is that the realistic conditions of lamination geometries, core materials, and winding connections are all considered collectively and faithfully. Figs. 6(a) and (b) show the self- and the mutual-flux linkages respectively.

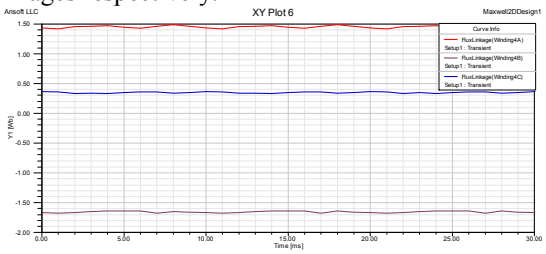

(a) self- flux linkage

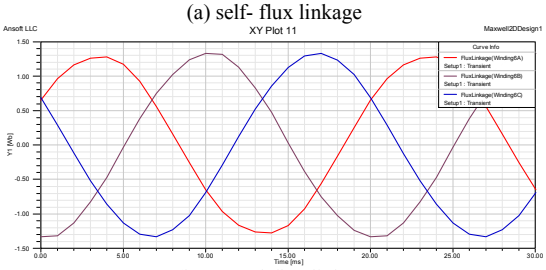

(b) mutual-flux linkage

Fig. 6 Self- and mutual-flux linkage versus rotor positions

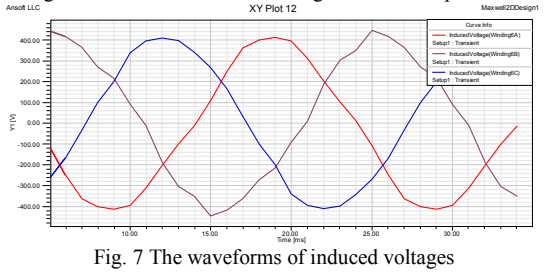

Fig. 7 The waveforms of induced voltages

As shown in Fig. 6(a), when the excitation current is DC, the self-flux linkage of the winding is also DC, independent of the rotor speed and positions. We can derive that if the RLMB-rotor DEBM is singly excited; no flux linkage variation will be experienced by the excited winding. Thus, no induced speed voltage and no electromechanical energy conversion will be possible. In addition, AC excitation on one set of stator windings also gives the same conclusions.

From Fig. 6(b), it very important to note that the mutual-flux linkage is closely related to the rotor positions. In effect, Eq. (2) relating the frequencies ω_1, ω_2 and ω_m is fully verifiable by the figure. Under such circumstances a speed voltage will be induced in the other set windings while the rotor is moving. Further, the profile of the mutual-flux linkage indicates that the induced speed voltage will be sinusoidal.

Fig. 7 shows the waveforms of induced voltages at one current level. The sine wave shape of the induced voltages is verified. All calculation results of induced voltage are summarized into the magnetizing curves shown in Fig.10. It is evident that the two sets of stator windings do emulate the functions of the stator and rotor windings respectively in a conventional doubly fed induction machine.

D. Torque Capability

In RLMB-rotor DEBM, when one set of stator winding is excited by DC or AC, Back EMF voltages will be induced in another set of stator windings, due to mechanical rotation of the RLMB-rotor. The general form of the torque is

$$T_e = \frac{3E_p I_p \cos\varphi + 3E_q I_q \cos\varphi}{\omega_{rm}} = \frac{3\omega_1 \lambda_{mq} I_p \sin\varphi + 3\omega_2 \lambda_{mp} I_q \sin\varphi}{\omega_{rm}} \quad (3)$$

$$= \frac{3}{2}(p+q)\lambda_{mq} I_p \sin\varphi$$

where the E_p and E_q, are the induced back EMF, the speed voltages associated with the variations of the mutual flux linkages; I_p and I_q are the phase currents; φ is the angle between the induced speed voltages and the current; λ_{mp} and λ_{mq} are the mutual flux linkages under the given currents. Note that if the phase current is injected in phase with respect to the induced speed voltage, or equivalently, orthogonal to the variation of the mutual-flux linkage of the non-excited winding, a maximum torque production for the given currents is expected.

The finite element analysis is used to calculate torque production of the designed DEBM. Fig. 8(a) shows the torque production curves computed directly by finite element method at one current levels of the sample DEBM. In the calculation, both sets of the stator windings are excited with frequencies conforming to Eq. 2. At the same time the relative phase angles are changed as a parameter of the torque production. The torque production by finite element analysis is directly based on the magnetic field density and intensity on each element. The results are considered accurate because the complicated geometry of the DEBM and nonlinearity of the materials are full considered. The torque production of the RLMB-rotor DEBM operated at the rated current levels and 600rpm as a function of the phase angle between the two sets of stator windings are shown in Fig. 8 (b).

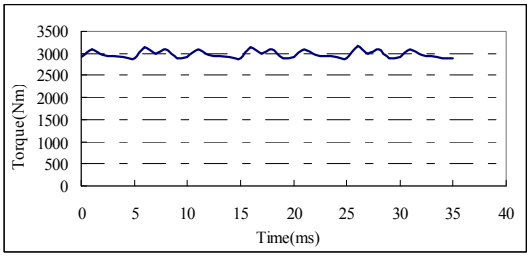

(a) Torque versus time

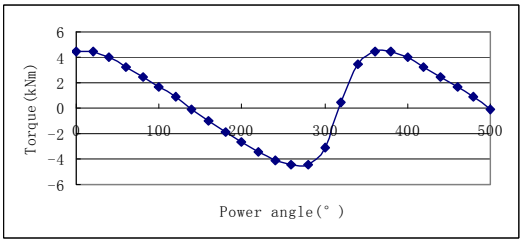

(b) Torque angle characteristics

Fig. 8 Torque characteristic

III. EXPERIMENTAL TESTING RESULTS

Experiments have been carried out on the built 250kw/1200rpm DEBM in the laboratory. Fig. 9 shows the pictures of the stator, the RLMB-rotor and the DEBM respectively. The open-circuit experiment and doubly excited operation experiments are carried out in laboratory, the frequency of the power grid is 50Hz, so the natural synchronous speed of the sample machine is 600rpm.

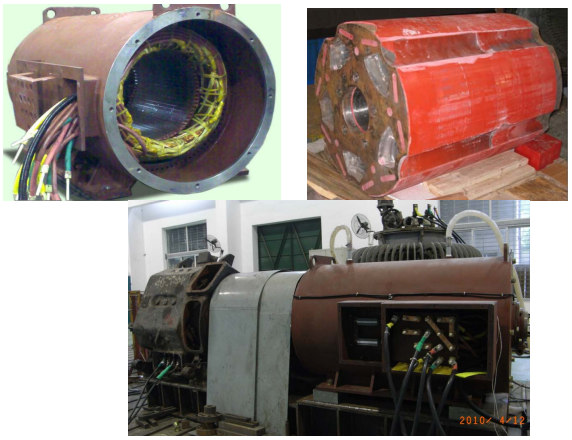

Fig. 9 Pictures of the prototype DEBM

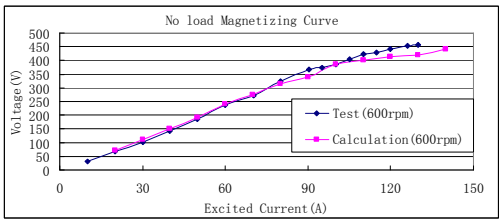

Fig. 10 No-load magnetizing curve

Fig. 10 shows the open-circuit characteristic comparison of the prototype RLMB-rotor DEBM between FEM and experimental results. From the no-load characteristics, we can find that the experimental results and the design results are satisfied very well.

Fig. 11 shows the experiment system schematic diagram for double-excited operation mode. The experiment results are collected at power grid side and the primary winding side of the DEBM by using two types of measure means, one means is to collect the waveform of the voltage and the current, the other is to collect the power directly. Table 2 lists the efficiency comparison of the DEBM system and the test data are collected at dot1 shown in Fig. 11. Table 3 lists the collection results and calculation results of the DEBM at dot2 shown in Fig. 11. Fig. 12(a), (b) show the waveform at dot 1 and dot 2 in same operation mode respectively.

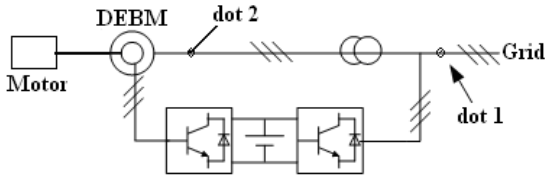

Fig. 11 Schematic diagram of DEBM experiment system

TABLE 2 TEST RESULTS OF DOT #1

Input		Means #1 results		Means #2 results	
i_{rq}	P_1(kW)	P_{01}(kW)	η	P_{01}(kW)	η
-0.3	94	87.76	0.9337	87.5	0.9309
-0.4	131	123.04	0.9392	122	0.9313
-0.5	160	148.16	0.9260	148	0.9250

TABLE 3 TEST RESULTS OF DOT #2

i_{rq}	U(V)	I(A)	cosφ	P_{02}(kW)
-0.3	452.62	111.74	0.753	56.13
-0.4	452.62	135.79	0.794	86.58
-0.5	459.7	157.00	0.8662	103.14

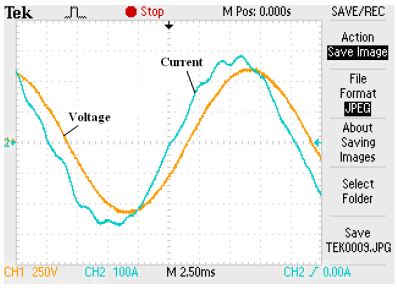

(a) dot 1 (i_{rq}=-0.3)

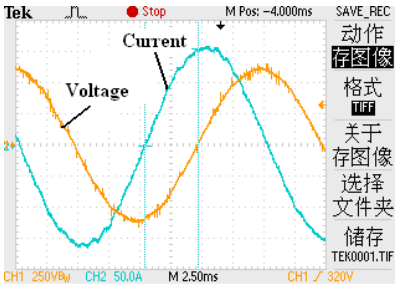

(b) dot 2(i_{rq}=-0.3)

Fig. 12 Waveform of the system

From Table 2, we can find that the efficiency of the DEBM measured by two means is much closed, and the efficiency of the whole system achieves 92% in minimum. If the converter losses (2%) and the booster losses (2%) are take into account, the individual efficiency of the prototype DEBM will achieve 95%, all these show that the designed prototype DEBM with RLMB-rotor are potential to achieve high efficiency operation.

From Table 3, if the ratio of the active and the reactive current is changed, the power factor of the prototype DEBM will change correspondingly, these show that the power factor of the prototype DEBM can be controlled flexibly, and the power factor can achieve 1 or -1 when appropriate control methods are applied on the system. The prototype DEBM are potential to apply in variable speed constant frequency operation system.

IV. CONCLUSIONS

This paper focuses on the performance analysis of a prototype RLMB-rotor DEBM (250kW/1200rpm) for variable speed system. The magnetic fields distribution, the torque characteristics and the experimental results of the prototype machine are presented. The studies show that the RLMB-rotor DEBM is potential to achieve high efficiency and apply in variable speed system.

V. REFERENCES

[1] L.J. Hunt, "The Cascade Induction Motor", J. IEE Vol. 52, 1914, pp. 406-426.

[2] A.R.W. Broadway, "Cageless Induction Motor", Proc. IEE, Vol. 118, 1971, pp.1593-1600.

[3] L. Xu, F. Liang, and L.Ye, "Comparison Study of Rotor Structures of Doubly Excited Brushless Reluctance Machine by Finite Element Analysis", IEEE Transactions. On Energy Conversion, Vol. 9, No. 1, March, 1994, pp165-172.

[4] L. Xu and F. Wang, "Comparative study of magnetic coupling for a doubly fed brushless machine with reluctance and cage rotors", Thirty-Second IAS Annual Meeting, IAS '97., Conference Record of the 1997 IEEE Vol. 1, Oct. 1997 pp.326-332.

[5] Fengxiang Wang and Fengge Zhang Longya Xu, "Parameter and Performance Comparison of Doubly-Fed Brushless Machine with Cage and Reluctance Rotors",IEEE Transactions on Industry Applications, Sep/Oct 2002, Vol.38, No.5, pp: 1237-1243.

[6] L. Xu, F. Liang and T.A. Lipo, "Transient Model of a Doubly Excited Reluctance Motor IEEE Transactions on Energy Convemion". Vol. 6, No. 1, March 1991, pp. 126-133.

[7] L. Xu, "Analysis of a Doubly-Excited Brushless Reluctance Machine by Finite Element Method", IEEE Industry Application Society Annual Meeting, 1992, Houston, Vol.1, pp.171-177.

[8] Y. Liao, L. Xu and L. Zhen, "Design of a doubly fed reluctance motor for adjustable-speed drives", IEEE Transactions on Industry Applications, Vol. 32, No. 5, 1996, pp. 1195-1203.

[9] L. Xu, F. Liang and T. A. Lipo, "Analysis of a New Variable Speed Doubly Excited Reluctance Motor", Electric Machines and Power Systems, Vol. 19. No. 2, March 1991, pp. 125-138.

[10] R. Li, A. Wallace, and Rene Spee, "Dynamic Simulation of Brushless Doubly-Fed Machines", IEEE Transaction on Energy Conversion, Vol. 6, No. 3 September, 1991, pp.445-451.

[11] C.Brune, R. A. K. Wallace, "Experimental Evaluation of A Variable Speed Doubly-Fed Wind-Power Generation System," in Proc.1993 IEEE idustry Applications Society Conf., pp.480-487.

[12] Huijuan Liu and L. Xu, "Comparison study of Doubly Excited Brushless Reluctance Machine with different rotor pole numbers", International Conference on Power Electronics and Motion Control, 2009. IPEMC '09. Wuhan China. 17-20 May 2009, pp.830-835.